

Structural Indicators of Electronic Interaction in the 1,1',5,5'-Tetramethyl-6,6'-dioxo-3,3'-biverdazyl Diradical

David J. R. Brook, Harold H. Fox, Vincent Lynch, and Marye Anne Fox*

Department of Chemistry and Biochemistry, University of Texas at Austin, Austin, Texas 78712

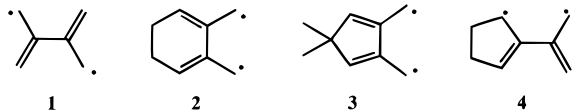
Received: June 6, 1995; In Final Form: September 25, 1995[⊗]

The diradical 1,1',5,5'-tetramethyl-6,6'-dioxo-3,3'-biverdazyl, **6**, crystallizes in a monoclinic unit cell with $a = 4.224(1)$, $b = 17.378(2)$, $c = 7.529(1)$ Å, $\beta = 96.02(1)^\circ$, space group $P2_1/c$ (No. 14). The crystal structure of **6** shows local D_{2h} symmetry. ESR measurements in a frozen chloroform solution indicate that isolated **6** has a singlet ground state with a triplet excited state 760 cm^{-1} (0.094 eV) above the ground state with zero-field splitting parameters $D = 0.038\text{ cm}^{-1}$ and $E = 0.0016\text{ cm}^{-1}$. Semiempirical calculations (AM-1) suggest that **6** is twisted in solution. Crystalline **6** shows a temperature-activated ESR signal with no features characteristic of an isolated triplet. Strong intermolecular π -stacking interactions prevent the analysis of this temperature activation in terms of intermolecular and intramolecular exchange parameters.

Introduction

The interaction between unpaired electrons is an important contributing factor governing the properties of many organic solids. Electron-coupling interactions are directly responsible for superconductivity and magnetism and have important consequences on the behavior of conductors and semiconductors. The study of stable biradicals with closely spaced and/or conjugated radical centers provides a useful starting point for the investigation of intramolecular electronic interactions. By studying such materials, it may be possible to build up a set of empirical structure–property relationships that can be correlated with, and used to improve, theoretical descriptions.

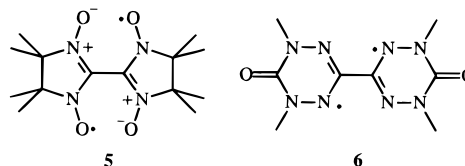
Many recent studies have focused on paramagnetic centers linked “meta through benzene”.¹ These systems are predicted, and found, to show ferromagnetic exchange between spins giving rise to high-spin ground states. A second group of structures are the disjoint, even alternant systems typified by the hydrocarbon tetramethylene ethane **1**, TME.



Disjoint biradicals are formally derived from the connection of two radicals at a point where each radical has a node in its SOMO. In the resulting molecules the two nonbonding molecular orbitals, and hence the unpaired electrons, can be confined to separate regions of the molecule. Coupling between the two unpaired electrons is predicted to stabilize a singlet ground state,^{2,3} but currently available experimental data on biradical hydrocarbons refutes this prediction. TME itself appears to have a triplet ground state⁴ but probably has a twisted D_{2d} conformation.⁵ The related biradical 2,3-bis(methylene)-1,3-cyclohexadiene, **2**, has a nearly planar triplet ground state⁶ and the biradicals 2,2-dimethyl-4,5-bis(methylene)-1,3-cyclopentadiene,⁷ **3**, and 2-(1-methyleneethenyl)cyclopentenyl,⁸ **4**, both probably have triplet ground states. The dianion of 9,9'-bianthryl has been reported to have a triplet ground state⁹ with a D_{2d} geometry. This result has been rationalized in terms of the zero overlap between perpendicular π systems and suggests that *p*-phenylene systems should also show high-spin ground

states when doped.¹⁰ Contrary to the results for these hydrocarbons, the heteroatom analog bis(nitronyl nitroxide) **5** is twisted about the central bond and has a singlet ground state.^{11,12} In each of these systems, the lowest singlet and triplet states are close in energy and confident prediction of the ground-state multiplicity is clearly challenging. The continued investigation of these and related systems is important to help clarify the nature of these electronic interactions.

Biradical **6**, whose ESR and absorption spectra were first reported in 1980 by Neugebauer,¹³ can be considered a heterocyclic analogue of TME. Determination of the ground-state multiplicity and conformation of **6** are important in further elucidating the nature of electronic interactions in disjoint biradicals. We report here the crystal structure, electronic structure, and solution- and solid-state ESR spectra of **6**.



Results

The diradical **6** was obtained^{13,18} as very dark red-black crystals. Aerated solutions of **6** in organic solvents were found to decompose slowly at room temperature; consequently, as a precaution, samples were handled under nitrogen. Crystals were grown by slow diffusion of THF into a chloroform solution of **6**. Several crystal morphologies were observed, including needles and rhombi; however, X-ray analysis revealed that all morphologies had the same monoclinic unit cell. Solution of the X-ray data gave the structure depicted in Figure 1.

The planar structure of the molecule is surprising. Lone pair–lone pair repulsion would be expected to stabilize a twisted structure for **6**; indeed, semi-empirical (AM1) calculations on **6** suggest a bond order of 0.94 for the central C–C' bond and a twist angle of 86° in a geometry optimized structure. Though AM1 calculations have been shown to overestimate lone pair repulsion in 2,2'-bipyrimidine,¹⁴ the qualitative prediction of a twisted conformation is still valid. A plot of the dependence of the heat of formation on inter-ring dihedral angle suggests that although a twisted conformation is preferred, the minimum is very shallow (Figure 2). The twisted conformation is

[⊗] Abstract published in *Advance ACS Abstracts*, January 15, 1996.

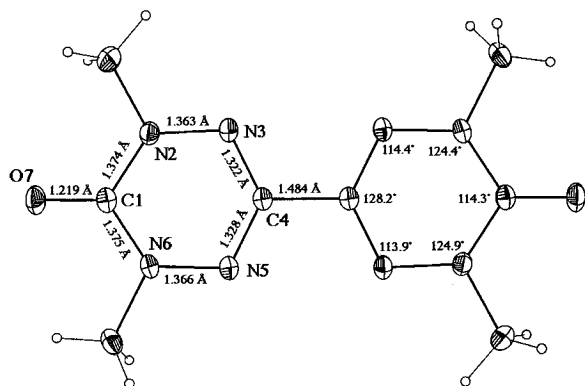


Figure 1. Thermal ellipsoid plot of **6** showing the atomic numbering scheme used for crystallography, as well as selected bond lengths and bond angles.

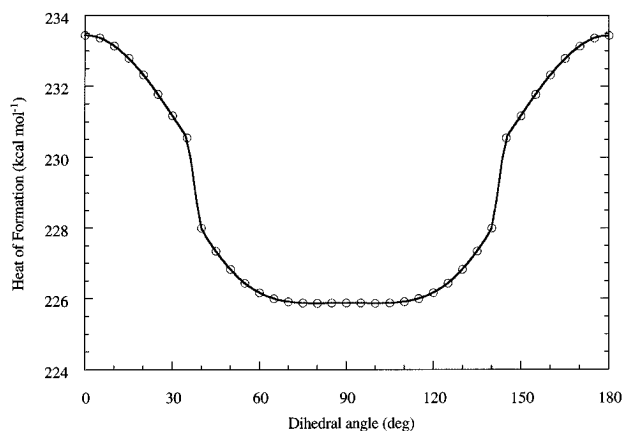


Figure 2. Dependence of the calculated heat of formation (AM1) of **6** on inter-ring dihedral angle.

calculated to be more stable than the planar form by 7.6 kcal mol⁻¹. This result strongly suggests that although the molecule is planar in the crystal, this preference likely depends on packing forces independent of the preferred geometry for electronic interactions and it is certainly likely to adopt a twisted structure in solution when such packing forces no longer dominate.

With an assumed planar structure like that observed in the solid state, selected energy levels could be calculated from the AM-1 parameters employing a restricted Hartree-Fock basis set (Figure 3). These calculations predict the molecular orbitals to be nearly identical in the singlet and the triplet. In addition the HOMO and LUMO are very similar to those of TME³ modified by the additional bonding and antibonding interactions with the other sp²-hybridized atoms in the ring system. The total energy of the singlet is higher than that of the triplet by 2.1 eV (47 kcal mol⁻¹), as determined by the RHF calculation. However, the results of UHF calculations indicate that the singlet state is more stable than the triplet by only 0.12 eV (2.8 kcal mol⁻¹). The results of the UHF calculations are consistent with the experimental findings presented below.

Chloroform solutions of **6** show absorption spectra identical to those reported earlier.¹³ Beer's law plots provide no evidence of molecular association in solution. At room temperature, solutions in degassed chloroform show a single, relatively broad (peak-to-peak line width of 3 mT) ESR signal with no hyperfine structure. As the solution is cooled below 250 K, the signal is resolved into a broad signal with highly temperature-dependent line width and a relatively narrow signal that exhibits hyperfine structure consisting of at least 15 lines with a spacing of 0.54 mT. The nature of the sharp signal was not determined but appears to result from chemical oxidation of **6**. The line width

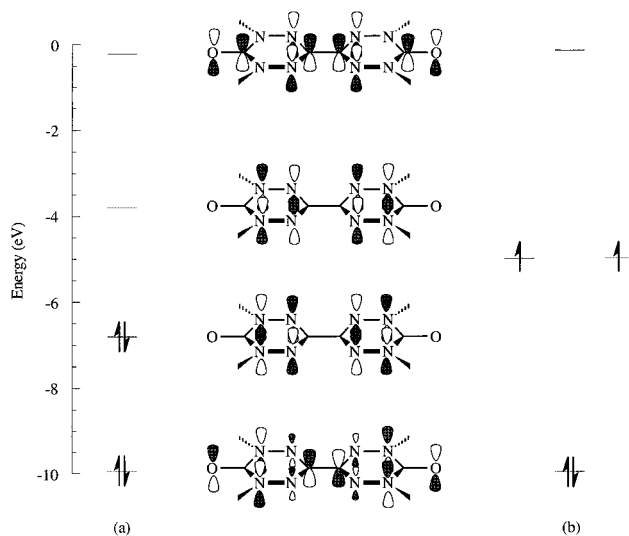


Figure 3. Energy levels calculated (RHF) using AM1 parameters for planar **6**: (a) as a singlet (total energy = -3475.3816 eV) and (b) as a triplet (total energy = -3477.4322 eV).

of the broad signal increases rapidly as T decreases, reaching a peak to peak line width of 20 mT at 210 K. This temperature dependence, along with the broad signal expected for a triplet in nonrigid media, leads to assignment of this signal to the triplet state of **6**. Upon freezing of the solution, a spectrum characteristic of a randomly oriented triplet with no hyperfine structure is observed (Figure 4). The spectrum shows no hyperfine structure. Assuming an isotropic g value,¹⁵ analysis of the spectrum yields the zero field splitting parameters, $|D| = 0.038$ cm⁻¹ and $E = 0.0016$ cm⁻¹. (The sign of D cannot be determined from the spectra of randomly oriented species except at extremely low temperatures.)

Zero-field splitting results from the magnetic dipolar interaction of the two unpaired electrons. The magnitude of the dipolar interaction depends strongly on magnetic field direction and interdipole distance. Consequently, the parameters D and E are strongly dependent on molecular symmetry and structure. A comparison of the observed values with those calculated from molecular orbital coefficients using a point dipole approximation can, in favorable cases, give some indication of preferred molecular conformation.^{12,16,17} Figure 5 shows the calculated dependence of the zero field splitting parameters D and E , as a function of twist angle, α , with the orbital coefficients obtained from the triplet AM1 calculation. Unfortunately, the predicted absolute value of D is much lower than the observed one and varies little with molecular conformation: the observed variation is considerably less than the estimated error in the calculation. The predicted dependence of E on dihedral angle is considerably more sensitive to initial wave function than D ; hence an interpretation of the measured value through the calculations shown in Figure 5 is risky. The approach of E to zero as α approaches 90° is a feature required by symmetry. Consequently, the measured non-zero value of E eliminates the possibility of a D_{2d} ($\alpha = 90^\circ$) conformation for **6** in chloroform solution. In benzene, Neugebauer reports $|D| \approx 0.030$ cm⁻¹, $E \approx 0$ cm⁻¹ for **6**.¹⁸ These values are very close to those calculated for a D_{2d} geometry. This suggests that the molecular orbital calculations are a good model for **6** in environments with weak solvent interactions but that significant perturbation of the conformation and electronic structure occurs through interaction with solvent molecules.

Inspection of the low-field region of the ESR spectrum reveals a half-field signal corresponding to transitions between the $m_s = -1$ and $m_s = +1$ states of the triplet. The temperature

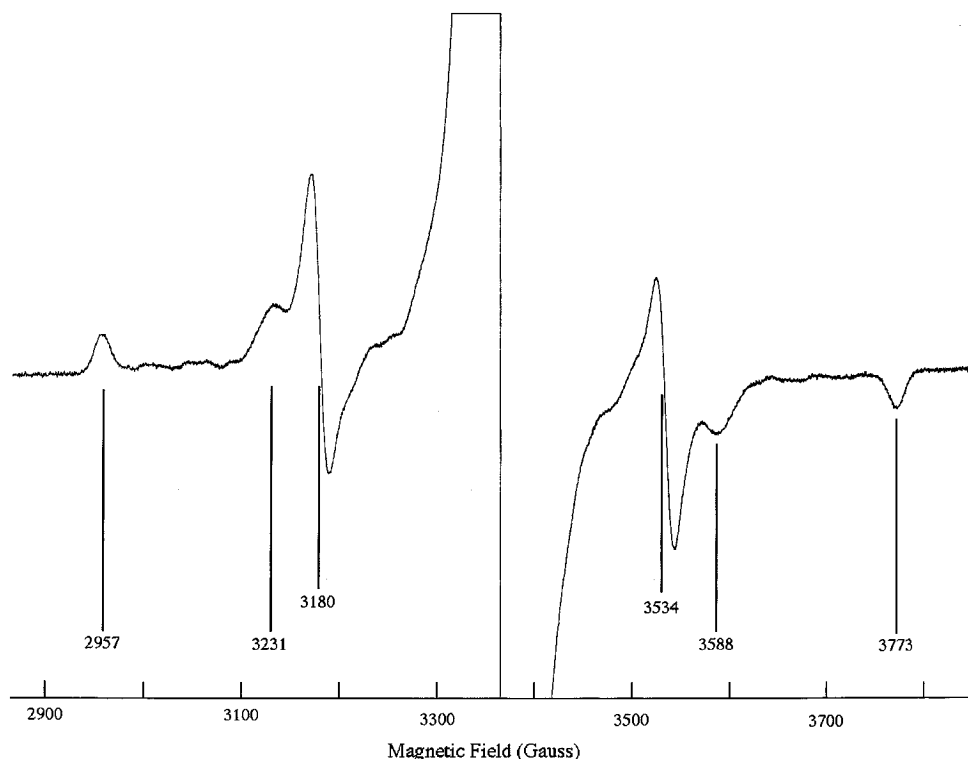


Figure 4. ESR spectrum of **6** in frozen chloroform at 200 K. The large central peak is due to a trace doublet impurity from the air oxidation of **6**.

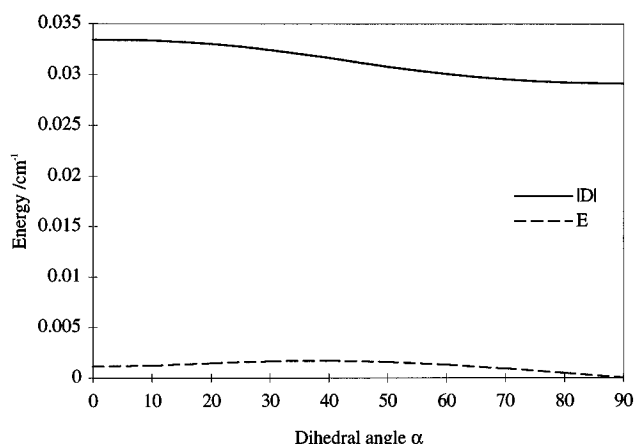


Figure 5. Dependence of the AM-1 calculated absolute values of the zero-field splitting parameters D and E , on ring-ring dihedral angle, α . The sign of D is calculated to be negative.

dependence of this signal allows the determination of the ground-state multiplicity and the singlet-triplet energy separation J . This method is preferred over measurement of the intensity of the $\Delta m_s = 1$ transitions, since the half-field region has no interfering absorbances from doublet species. The half-field signal of **6** shows strong temperature activation, indicating a singlet ground state. Fitting the temperature dependence of the intensity of the half-field signal to the Bleay-Bowers equation (Figure 6)¹⁹ gave a singlet-triplet energy separation J of 760 cm^{-1} (0.094 eV).

In solution, the conformation of **6** is probably twisted with D_2 symmetry. In the solid state, the conformation is fixed with local D_{2h} symmetry. This change in conformation is almost certainly a result of strong intermolecular interactions within the crystal lattice. The packing diagram (Figure 7) clearly indicates strong π -stacking interactions. Molecules are arranged into infinite stacks with a separation between molecular planes of 3.21 \AA . The molecules are tilted through 50° from the

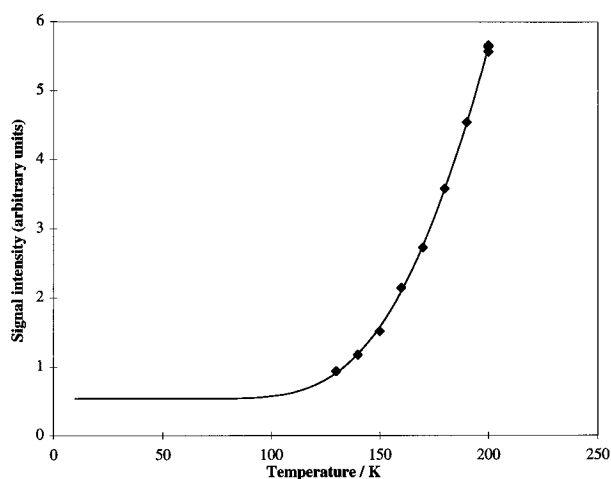


Figure 6. Temperature dependence of the half-field signal intensity for **6** in frozen chloroform solution. The solid line is a best fit to the modified Bleay-Bowers equation $I = (q/T)/(3 + e^{J/k_B T}) + p$ with parameters $J = 760 \text{ cm}^{-1}$, $q = p = 0.5$.

stacking axis, giving a herringbone structure. The central C-C' bond in each molecule overlaps with an N-N group from each neighboring molecule in the stack.

The effect of these π -stacking interactions is clearly seen in the optical absorption spectrum of the solid. A potassium bromide pellet containing **6** clearly shows a long absorption tail extending into the near-IR. The ESR spectrum of the solid also reveals strong intermolecular interactions. Both single crystals and polycrystalline samples of **6** at room temperature show a narrow (full width at half-maximum line width of 15 G) ESR line at $g = 2.0014$. The g value is very close to isotropic. No hyperfine splitting nor zero-field splitting effects are seen, nor is a half-field transition observed. The signal is strongly thermally activated, with the temperature dependence of χ_N (the normalized susceptibility, determined from ESR signal intensity) and $\chi_N T$, being plotted in Figure 8. After compensat-

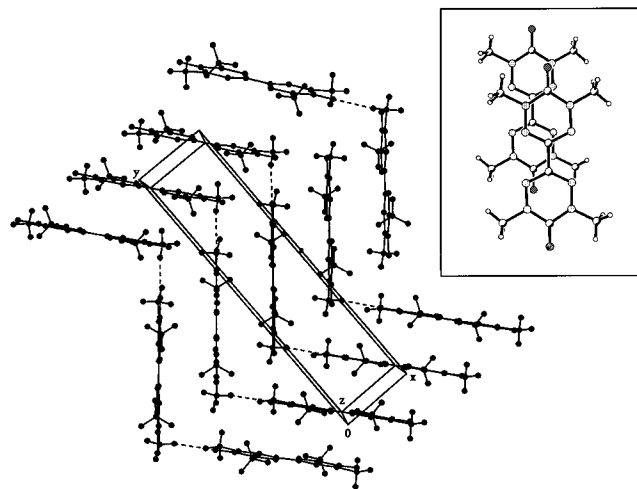


Figure 7. Packing diagram and unit cell for **6**. The view is along the *c* axis. The inset shows the overlap between neighboring molecules in a stack.

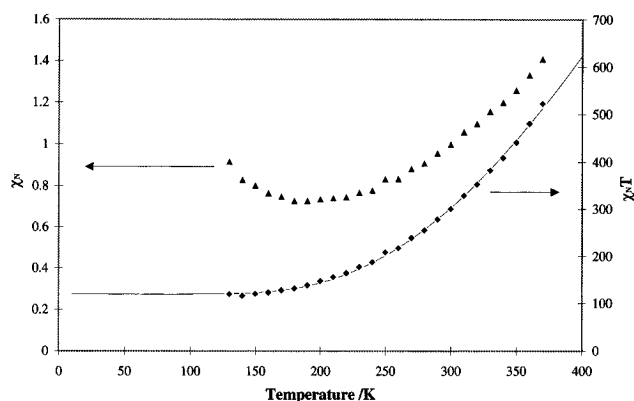


Figure 8. Dependence of the normalized susceptibility χ_N (▲) and the product of susceptibility with temperature $\chi_N T$ (◆) on temperature. The solid line is a best fit to the function $\chi_N T = ke^{-\Delta E/k_B T} + p$ with $\Delta E = 0.11$ eV, $k = 10370$, $p = 120$.

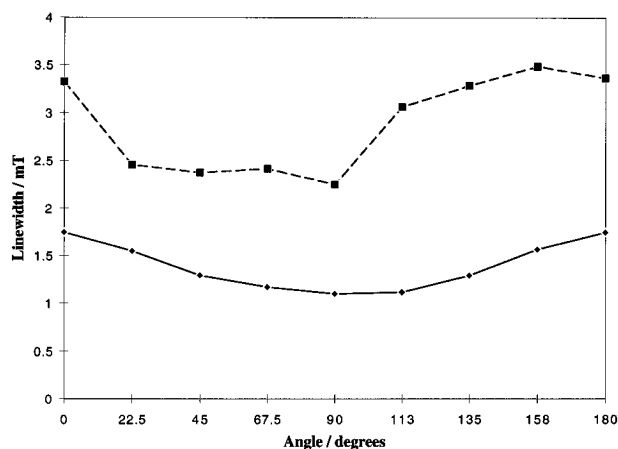


Figure 9. ESR line width (in mT) of a single crystal of **6** as a function of crystal orientation at 300 K (■) and 77 K (▲). An orientation with the crystallographic *a* axis oriented perpendicular to the magnetic field corresponds to 0° . The axis of rotation was not determined.

ing for Curie behavior (by plotting $\chi_N T$), the signal shows exponential behavior with an activation energy of 887 cm^{-1} (0.11 eV). The signal approaches a constant value as T approaches zero. The nature of this residual signal is clearly seen upon investigation of the angular dependence of the line width at room temperature and at 77 K (Figure 9). The 77 K signal shows a $(3 \cos^2 \theta - 1)$ angular dependence characteristic of dipole-dipole interactions, in this case probably caused by

anisotropic hyperfine coupling. Importantly, the angle of maximum low-temperature line width does not coincide with the symmetry axis of the crystal. This suggests that the observed low-temperature signal is caused by a doublet impurity incorporated into the lattice that remains after the excited ESR-active states have been depopulated. At room temperature, the line width is considerably narrower and shows an angular dependence that corresponds to the crystal symmetry. After determination of the activation energy, the ratio of signal intensities at low temperature and at room temperature can be used to estimate the concentration of this impurity as 1%.

Discussion

To a first approximation, **1** and **6** would be expected to show similar properties. Both molecules are anticipated to show twisted conformations and similar electronic structures. AM1 calculations show that the molecular orbitals in these molecules are closely related (Figure 3). In a frozen solution, the bis-verdazyl **6** shows strong antiferromagnetic coupling with the singlet lying 758 cm^{-1} (0.094 eV) below the triplet, as is predicted for disjoint π systems. The bis(nitronyl nitroxide) **5** also has a singlet ground state, though by a smaller margin of 306 cm^{-1} (0.038 eV). **1** and related hydrocarbon analogues (for which the prediction of singlet ground states were originally made) appear to show triplet ground states in both twisted and planar conformations, contradicting both the simple Borden-Davidson theory³ and high level calculations.⁵ Clearly, these systems are still only poorly understood.

As a further indicator of the complexities of these systems, we note that the zero-field splitting parameter D for **6** is anomalously large. The magnitude of D is proportional to $1/r^3$ where r is the average interspin distance. The measured D for **6** is almost twice that observed for **1**, implying that the spins are, on average, closer together, despite the fact that the more extended π system in **6** would be expected to allow the spins to stay further apart.

The planar structure of **6** in the solid state is remarkable but not without precedent. Biphenyl²⁰ and 2,2'-bipyrimidine²¹ are twisted in the gas phase but show planar conformations in the solid state. The crystal structures of these molecules show large librations about the central C-C' bond, suggesting either a statistical distribution of twisted states or a very low rotational energy barrier. 2,2'-Bipyrimidine hydrate, like **6**, shows a completely planar structure in the crystal. Presumably this is attained through the formation of hydrogen bonds with solvent. In solid **6**, intermolecular electronic interactions between the unpaired electrons favor a planar conformation. The activation energy for interaction between paramagnetic centers in crystalline **6** is clearly close to the value determined for the singlet-triplet splitting in solution and also close to the value calculated for planar **6**. It is tempting to interpret this energy as the singlet-triplet splitting for planar **6**, but this interpretation may be rather simplistic.

In interpreting these data, we must consider the relative magnitude of the intermolecular and intramolecular exchange terms. The domination of the intermolecular interactions dominate seems unlikely since the magnetic properties of the crystal would approximate two linear Heisenberg chains which have nonzero magnetic susceptibility even at 0 K.²² Furthermore, the magnitude of the intramolecular interaction is known to be large in solution.

A more reasonable model for these data assumes that intermolecular interactions are small and that the triplet states within the crystal (excitons) are extremely mobile. This model was proposed by Nordio and co-workers to describe the ESR

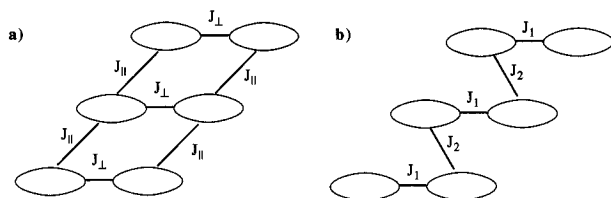


Figure 10. Possible magnetic interaction schemes in crystalline **6**. (a) Heisenberg ladder; (b) alternating Heisenberg chain. Each ellipse represents one verdazyl unit (i.e., one-half of molecule **6**).

spectral properties of certain TCNQ salts.²³ Rapid migration of the triplet excitons along the stack averages the hyperfine splitting to zero, whereas collision of excitons with the doublet impurity or with another exciton scrambles the electron spins through exchange and likewise averages the zero-field splitting to zero. In this model, the measured activation energy corresponds to the energy of a single exciton, which would approach that of the isolated, planar molecule as the intermolecular exchange is reduced.

Although the above model adequately explains the ESR data, it neglects the spectroscopic and crystallographic data obtained for crystalline **1**. The close spacing of neighboring π systems and the long-wavelength IR absorption both suggest that intermolecular interactions are important. Data from other systems indicates that the assumption of small intermolecular interactions is unjustified in describing π -stacked systems. In the π -stacked (TCNQ)₂²⁻ dianion, the two electrons can interact so strongly that the dimer is diamagnetic, even at room temperature.²⁴ The triplet exciton in tetraethylammonium tetracyanobenzoquinonide shows a singlet–triplet splitting of 0.38 eV,¹⁷ almost 4 times as great as that observed on monomeric **6**. This triplet results from the face-to-face interaction of two radical anions. Clearly, intermolecular interactions in **6** must be at least great enough to overcome the nitrogen lone-pair interactions and allow a planar conformation. For 2,2'-bipyrimidine, the energy required to achieve a planar conformation has been experimentally determined to be 1.5 kcal mol⁻¹,^{21b} in agreement with ab initio calculations.²⁵ AM1 calculations estimate that for **6** this energy is roughly 7.6 kcal mol⁻¹, based on the results summarized in Figure 2. Even with the lower value measured for bipyrimidine, these energies are comparable to the measured intramolecular exchange in solution. In light of this result, the assumption of negligible intermolecular exchange interactions is questionable.

If intermolecular interactions are of the same order of magnitude as intramolecular interactions, the concept of isolated triplets and singlets is no longer useful and more complex models are required. Two possible interaction schemes are the Heisenberg ladder²⁶ or the alternating one-dimensional Heisenberg chain²⁶ (Figure 10). Though numerical solutions are available for the magnetic susceptibility expected from each of these models, they both approximate a simple exponential function when $kT < J$. Fitting of the available data to these models does not allow distinction between them and does not lead to unique solutions. We also note that the exponential behavior of the susceptibility does not eliminate the possibility of planar **6** having a triplet ground state with strongly antiferromagnetic intermolecular coupling. Haldane²⁷ proposed that the magnetic susceptibility deriving from such a model would also show exponential behavior at low temperature.

Unfortunately, the complexity of the intermolecular interactions in this nondilute magnetic system prevent the determination of the value for intramolecular exchange for the isolated planar molecule. The strength of these interactions suggest, however, that neutral radicals such as **6** may provide a novel structural

unit for the synthesis of new organic magnetic and conductive materials. In this context, Dagotto and co-workers²⁸ proposed that a hole-doped Heisenberg ladder should show superconducting behavior.

Conclusion

Bisverdazyl **6**, in solution, shows a singlet ground state lying about 3 kcal mol⁻¹ below the lowest triplet. A singlet–triplet energy difference of 2.77 kcal mol⁻¹ was estimated from AM-1 calculations. Although this result is in agreement with theories proposed for disjoint diradicals, the range of results reported for conceptually similar molecules suggests that more elaborate theories may be required to reliably predict a priori the ground-state multiplicities of these molecules. The crystal structure of **6** shows that neutral diradicals can distort geometrically by forming strong intermolecular interactions through π stacking.

Experimental Section

Diradical **6** was synthesized using the procedure described by Neugebauer.¹⁶ To minimize the concentration of doublet impurities in the material, all manipulations of **6** were performed under a nitrogen in nitrogen purged solvents. Spectroscopic properties of **6** were as previously described.¹⁶

Crystallography. Very dark red lathe-shaped crystals were grown by layering a chloroform solution of **6** with THF and allowing the layers to diffuse together. The analyzed crystal had approximate dimensions of 0.14 × 0.25 × 0.43 mm. The data were collected at 173 K on a Nicolet P4 diffractometer, equipped with a Nicolet LT-2 low-temperature device and using a graphite monochromator with Mo K α radiation ($\lambda = 0.71073$ Å). Details of crystal data, data collection, and structure refinement are listed in the supporting information. Three reflections (1,5,-1; 0,2,3; 1,2,1) were remeasured every 97 reflections to monitor instrument and crystal stability. A smoothed curve of the intensities of these check reflections was used to scale the data. The scaling factor ranged from 1.00 to 1.02. The data were corrected for Lp effects but not for absorption. Data reduction and decay correction were performed using the SHELXTL-Plus software package.²⁹ The structure was solved by direct methods and refined on F^2 by a full-matrix least-squares fitting program³⁰ with anisotropic thermal parameters for the non-H atoms. The hydrogen atoms were located from a ΔF map and refined with isotropic temperature factors. The planar molecule lies on a crystallographic inversion center at $1/2, 1/2, 1/2$. The maximum deviation from planarity for a non-hydrogen atom is 0.01 Å for C8. The function $\sum w(|F_o|^2 - |F_c|^2)^2$ was minimized, where $w = 1/[(\sigma(F_o))^2 + (0.0528P)^2 + 0.0941P]$ and $P = (|F_o|^2 + 2|F_c|^2)/3$. Neutral atom scattering factors and values used to calculate the linear absorption coefficient are from the International Tables for X-ray Crystallography (1992).³¹ Computer programs used in data treatment have been described elsewhere.³² All figures were generated using SHELXTL-Plus.²⁹ Tables of positional and thermal parameters, bond lengths, bond angles, and torsional angles and lists of observed and calculated structure factors are listed in the supporting information.

Molecular Orbital Calculations. Semiempirical electronic structure calculations were carried out using MOPAC 6.00, as included in the CAChe 3.7 software package, running on a PowerMacintosh 8100/80. The AM1 parameters used in the calculations were taken from the literature.³³ Atomic coordinates used in the calculations were taken directly from the X-ray crystal structure data reported herein. Geometry optimization was achieved when the change in energy was less than 0.0002

kcal mol⁻¹. Singlet RHF, biradical RHF, UHF, and triplet UHF calculations were performed on the structure observed in the solid state.

ESR Spectroscopy. ESR spectra were recorded on a Bruker ESP300E X-band spectrometer equipped with a ER-4011 variable-temperature controller. Solution spectra were recorded using a saturated solution of **6** in argon purged chloroform. The intensity of the half field signal was obtained by double integration. Intensity data was fitted to the modified Bleany–Bowers equation

$$I = (q/T)/(3 + e^{J/k_B T}) + p$$

using a least-squares method to give the singlet–triplet separation J along with the proportionality constant q and the temperature-independent term p . The latter term was included to allow for errors in baseline integration. Measurements at 77 K were achieved by immersing the sample in a quartz liquid nitrogen Dewar flask that was designed specifically to fit within the spectrometer cavity. The single crystal for the VT study was glued to the end of a quartz rod with the a axis (needle axis) perpendicular to the rod. A marker glued to the rod indicated the orientation of the crystal within the cavity. The crystallographic axis parallel to the axis of rotation was not determined. VT measurements were taken with the crystallographic a axis perpendicular to the magnetic field. The normalized magnetic susceptibility, χ_N was calculated as

$$\chi_N = I/I_{300}$$

where I is the integrated signal intensity and I_{300} is the integrated signal intensity at 300 K. Data were fitted to the function

$$\chi_N T = ke^{(-\Delta E/k_B T)} + p$$

using a least-squares method to give ΔE and p where ΔE is the energy gap, k is a proportionality constant, and p is a constant related to the concentration of the doublet trace impurity.

Supporting Information Available: Full details of data collection parameters, tables of atomic coordinates, anisotropic thermal parameters, bond lengths, and bond angles for **6** (5 pages); list of observed and calculated structure factors (4 pages). Ordering information is given on any masthead page.

Acknowledgment. This work was supported by the National Science Foundation, the Texas Advanced Research Program, and the Robert A. Welch Foundation.

References and Notes

- (1) Dougherty, D. A., In *Research Frontiers in Magnetochemistry*; O'Connor, C. J., Ed.; World Scientific: London, 1993; p 327.
- (2) Hüchel, E. *Z. Phys. Chem.* **1936**, *34*, 339.
- (3) Borden, W. T.; Davidson, E. R. *J. Am. Chem. Soc.* **1977**, *99*, 4587.
- (4) Dowd, P.; Chang, W.; Paik, Y. H. *J. Am. Chem. Soc.* **1986**, *108*, 7416.
- (5) Nachtigall, P.; Jordan, K. D. *J. Am. Chem. Soc.* **1993**, *115*, 270.
- (6) Dowd, P.; Chang, W.; Paik, Y. H. *J. Am. Chem. Soc.* **1987**, *109*, 5284.
- (7) Roth, W. R.; Kowalczyk, U.; Maier, G.; Reisenauer, H. P.; Sustmann, R.; Müller, W. *Angew. Chem., Int. Ed. Engl.* **1987**, *26*, 1285.
- (8) Roth, W. R.; Ruhkamp, J.; Lennartz, H. W. *Chem. Ber.* **1991**, *124*, 2047.
- (9) Hoshino, H.; Kimamura, K.; Iwamura, I. *Chem. Phys. Lett.* **1973**, *20*, 193.
- (10) Müllen, K.; Baumgarten, M.; Tyutyulkov, N.; Karabunarliev, S. *Synth. Met.* **1991**, *40*, 127.
- (11) Alies, F.; Luneau, D.; Laugier, J.; Rey, P. *J. Phys. Chem.* **1993**, *97*, 2922.
- (12) Ullmann, E. F.; Boocock, D. G. B. *Chem. Commun.* **1969**, 1161.
- (13) Neugebauer, F. A.; Fischer, H. *Angew. Chem., Int. Ed. Engl.* **1980**, *92*, 761.
- (14) Fabian, W. M. F. *J. Comput. Chem.* **1988**, *9*, 369.
- (15) Although in practice some anisotropy in g is expected, the variation in g is extremely small for an organic triplet in comparison to the zero-field splitting and, to a first approximation, can be ignored.
- (16) Luckhurst, G. R.; Pedulli, G. F.; Tiecco, M. *J. Chem. Soc. B* **1971**, 329.
- (17) Hynes, R. C.; Krusic, P. J.; Preston, K. F.; Springs, J. J.; Williams, A. J.; Miller, J. S. *J. Am. Chem. Soc.* **1995**, *117*, 2547.
- (18) Neugebauer, F. A.; Fischer, H.; Seigel, R. *Chem. Ber.* **1988**, *121*, 815.
- (19) Bleany, B.; Bowers, K. D. *Proc. R. Soc. London* **1952**, *A214*, 451.
- (20) Charbonneau, G. P.; Delugeard, Y. *Acta Crystallogr. B* **1976**, *32*, 470.
- (21) (a) Barone, V.; Cauletti, C.; Lejl, F.; Piancastelli, M. N.; Russo, N. *J. Am. Chem. Soc.* **1982**, *104*, 4571. (b) Fernholt, L.; Romming, C.; Samdal, S. *Acta Chem. Scand.* **1981**, *A351*, 707.
- (22) Bonner, J. C.; Fisher, M. E. *Phys. Rev. A* **1964**, *133*, 768.
- (23) Nordio, P. L.; Soos, Z. G.; McConnell, H. M. *Annu. Rev. Phys. Chem.* **1966**, *17*, 237.
- (24) Brook, D. J. R. Ph.D. Thesis, University of Colorado, 1993.
- (25) Barone, V.; Cauletti, C.; Piancastelli, M. N.; Ghedini, M.; Toscano, M. *J. Phys. Chem.* **1991**, *95*, 7217.
- (26) (a) Troyer, M.; Tsunetsugu, H.; Würtz, D. *Phys. Rev. B* **1994**, *50*, 13515. (b) Barnes, T.; Riera, J. *Phys. Rev. B* **1994**, *50*, 6817.
- (27) Haldane, F. D. M. *Phys. Lett.* **1983**, *93A*, 464.
- (28) Dagotto, E.; Riera, J.; Scalapino, D. J. *Phys. Rev. B* **1992**, *45*, 5744.
- (29) Sheldrick, G. M. SHELXTL-PLUS, Version 4.1. Siemens Analytical X-ray Instruments, Inc.: Madison, WI, 1990.
- (30) Sheldrick, G. M., private communication.
- (31) *International Tables for X-ray Crystallography*; Wilson, A. J. C., Ed.; Kluwer Academic Press: Boston: 1992; Vol. C, Tables 4.2.6.8 and 6.1.1.4.
- (32) Gadol, S. M.; Davis, R. E. *Organometallics* **1982**, *1*, 1607–1613.
- (33) Dewar, M. J. S.; Zuebisch, E. G.; Healy, E. F.; Stewart, J. J. P. *J. Am. Chem. Soc.* **1985**, *107*, 3902.

JP951573E